Oscillatory Packing and Depletion of Polyelectrolyte Molecules at an Oxide−Water Interface

Simon Biggs,*,† Raymond R. Dagastine,‡ and Dennis C. Prieve‡

SRC for Multiphase Processes, School of Environment and Life Sciences, Chemistry Discipline, The University of Newcastle, University Drive, Callaghan, NSW 2308, Australia, and Colloids, Polymers and Surfaces Program and Department of Chemical Engineering, Carnegie-Mellon University, Pittsburgh, Pennsylvania 15213

Received: July 2, 2002; In Final Form: August 27, 2002

Total internal reflection microscopy (TIRM) has been used to study the interactions between a 5 μm borosilicate glass sphere and a silica slide in the presence of a nonadsorbing polyelectrolyte, sodium (polystyrene sulfonate) (NaPSS). The effect of the polymer concentration, within the dilute solution regime, on the observed interactions was investigated. In all cases, the interactions displayed a short-range electrostatic repulsion followed immediately, at larger separations, by a decaying oscillatory interaction that is attributed to structuring of the polyelectrolyte in solution. The periodicity of the oscillations, as a function of concentration, indicates that at large surface separations the polymer chains are ordered as a nonintermixing, space-filling, latex. At polymer concentrations of between 200 and 1000 ppm, a transition to a system of ordered rods, parallel to the interface was seen for the final layer of polymer molecules.

1. Introduction

Polymers are routinely used to control the physical properties (i.e., stability and viscosity) of colloidal dispersions. Such control is vital to an enormous range of modern products and processes. Examples include cosmetics, explosives, water treatment, minerals processing, foodstuffs, paints, and inks, to name but a few.[1] As a result, the study of polymers both in solution and at interfaces has generated much interest over an extended period.[2]

The control of colloid stability has focused to a large extent on polymers that adsorb at an interface. Nonadsorbing polymers have typically generated less interest although the effects of such polymers upon colloid stability have been investigated continuously since the first reported experiments by Asakura and Oosawa in 1954.[3] Typically, nonadsorbing polymers will induce instability in a colloid dispersion at low polymer concentrations. The origins of this particle flocculation, which is commonly referred to as depletion, are found in the exclusion of polymer coils from between particles as they collide. Exclusion of the polymer during collision is driven by a restriction of the polymer coils configurational entropy at surface separations that are less than the characteristic size of the polymer in solution (i.e., 2 Rg). The exclusion of polymer from this gap leads to a local region, between the particles, which is solvent-rich. This, in turn, leads to a net osmotic pressure difference with the bulk that drives the particles together. Several theoretical models have been developed to explain the results from numerous experimental investigations of this depletion interaction at low polymer concentrations.[4−6] The situation is more complex as the polymer concentration is increased above the chain overlap concentration, c^*, into the semidilute and concentrated regimes. Under these conditions, a re-stabilization of the colloid dispersion has been predicted. Initial models suggested the origins of this depletion stabilization were from the development of a secondary barrier to flocculation.[1,7] More recently, van der Gucht and co-workers[8] have presented theoretical results that suggest the possibility of surface-mediated oscillatory packing of polymer chains at a solid−liquid interface. The system modeled in this study was a nonionic polymer at an uncharged surface. Under these conditions, oscillations were only observed in concentrated polymer solutions and the magnitude was dependent upon the solvent quality.

In aqueous colloid dispersions, control of stability is frequently generated using a polyelectrolyte. The choice of polyelectrolyte is typically governed by practical considerations because their properties may be subtly varied through parameters such as solution pH, salt concentration, and polymer charge (type and density). Development of comprehensive theories for polyelectrolytes in solution and/or at an interface is relatively immature when compared to their uncharged analogues.[9] This is primarily due to the far greater complexity of these systems. Depletion effects that are generated by polyelectrolytes interacting with colloid particles in an aqueous dispersion are one such example of a complex system. However, the importance of polyelectrolytes to colloid processing in areas such as wastewater treatment, minerals processing and food processing is a considerable spur to further research.

Depletion forces are typically small in magnitude. As a result, direct measurement of the force of interaction between two surfaces, or colloids, in the presence of nonadsorbing polymers has proven difficult. Development of increased measurement sensitivity during the past decade has resulted in a number of reports in the literature of direct measurements of depletion interactions. Such measurements have now been reported using the surface forces apparatus (SFA),[10] atomic force microscope,[11−16] and total internal reflection microscopy (TIRM).[17−19] Systems examined include particles,[17] micelles,[10] nonionic polymers,[11] highly charged polyelectrolytes,[12,15,16] a weak polyacid,[13,14] and a synthetic clay.[19] These investigations have confirmed the main features of the expected depletion interaction.

In simple depletion theories, such as that proposed by Asakura and Oosawa (AO),[20] it is assumed that the density distribution

* To whom correspondence should be addressed.
† The University of Newcastle.
‡ Carnegie-Mellon University.

10.1021/jp026425k CCC: $22.00
Published on Web 10/10/2002

of the depletant in the bulk, $\rho(r)$, is a constant. Under this limitation, depletant molecules (or particles) of radius r are displaced from the region between two approaching surfaces when the separation distance decreases to $D < 2r$. This generates a density gradient, and hence osmotic pressure, within the bulk fluid that can "push" the surfaces together. Hence, when $D < 2r$, the AO model predicts a monotonically attractive interaction potential. At low concentrations of depletant, this simple model accounts very accurately for the observed interaction. When the depletant molecules are sufficiently concentrated, liquid-structural correlations can occur, and these can significantly perturb the depletion attraction. The net result is an oscillatory interaction potential between two approaching surfaces. Such oscillatory interactions have been observed for particulate, micellar, and polymeric depletants.[10,12,15,21−25] In general, the sensitivity of the measurements allowed two, or at most three, oscillations to be observed. In the case of a polyelectrolyte depletant, addition of salt to the solution resulted in the oscillatory interactions diminishing in size and eventually disappearing.[12] The periodicity of the oscillations is related directly to the length scale of characteristic correlations within the bulk of the solution; for particles or micelles, this is their diameter, and for semidilute polymer solutions, it is the so-called "mesh-size". [26] Milling[12] demonstrated clearly that, across a wide concentration range, the periodicity of the oscillations as a function of concentration scaled like $c_p^{-1/2}$. After these original reports, further polymer systems have been investigated using AFM.[13−16] The basic conclusions regarding scaling correlations of the oscillations in the semidilute concentration regime and the role of salt have been confirmed.

In a series of related investigations, the influence of highly charged polyelectrolytes on the stability of thin liquid films has been investigated.[27−31] The presence of oscillatory force interactions in these systems was also reported. In the semidilute concentration regime for the polyelectrolytes used, the oscillations were observed to scale with concentration in a similar way to that described by Milling. This suggests that the origin of these interactions is similar in both cases, regardless of whether we have a solid or liquid interface. A complication of the liquid film studies is the requirement of having surfactant present to ensure film stability. Despite this problem, oscillatory interactions have been seen across a wide range of polymer/surfactant mixtures.[31] The reported oscillatory interactions using the thin film balance have been confirmed for similar polymer/surfactant systems at the solid−liquid interface using the SFA.[22,33]

To date, all of the reported investigations into oscillatory interactions generated by polymeric depletants have concentrated on the semidilute concentration regime. Milling and co-workers[13,15] have presented limited results within the dilute regime although no clear correlations can be discerned from the data. Direct measurement of the interparticle arrangement of polyelectrolyte molecules in salt-free or low salt conditions is a topic of great interest. The great majority of reported research has been undertaken using scattering techniques; either light, X-ray, or neutron.[9] Peaks in the scattering intensity as a function of q, the scattering wave vector,[34] are interpreted in terms of possible solution structures. In the dilute solution regime, conclusive evidence for the presence of solution structure, and its form (i.e., close packed rods or spheres), has been difficult to obtain. This is primarily related to the weak scattering observed from salt-free polyelectrolyte systems.

In this paper, we utilize the greater sensitivity afforded by the TIRM technique to undertake a detailed study of oscillatory interaction forces between two oxide surfaces in the presence of a highly charged polyelectrolyte, poly(styrene sulfonate), in the dilute solution regime. The data obtained are compared to standard scaling theories for salt-free polyelectrolyte solutions. The influence of the surfaces on solution ordering, and the effects of confinement between surfaces, are also discussed.

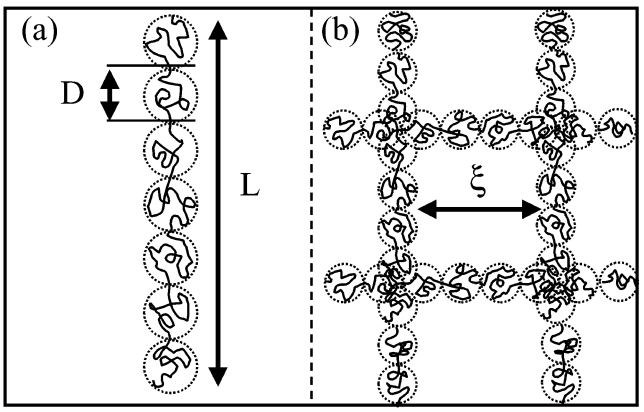

Figure 1. Schematic representation of polyelectrolytes in solution. (a) Dilute solution regime, where L is the characteristic rod length and D is the size of an electrostatic blob. (b) Semidilute solution regime, where polymer chains overlap with a characteristic mesh spacing of ξ.

2. Scaling Theory

The development of theories to describe the bulk solution behavior of polyelectrolytes has a long history.[9] The development of scaling theory, and its application to polyelectrolyte solutions, led to a convenient description of many concentration dependent solution parameters (e.g., coil size and viscosity).[26,35] In particular, the dependence of these parameters within the dilute, semidilute, and concentrated solution regimes, as well as a description of the phase boundaries has been achieved. A brief outline of the pertinent components of the scaling theory for linear polyelectrolyte solutions is given in this section.

In a dilute solution of a highly charged polyelectrolyte, the extension of any chain is controlled by electrostatic repulsions between nearest neighbor functional groups along that chain. Local electrostatic considerations result in a considerable amount of counterion condensation on any chain. Using the notation of Dobrynin et al.,[36] a polyelectrolyte solution, at a concentration of c monomers per unit volume, consists of chains having a degree of polymerization N and a monomer size b. Assuming that the monomer and counterion charges are univalent, the average number of monomers between charges is given as A and the total charge on a chain is therefore N/A. In dilute solution, a polyelectrolyte molecule is modeled as a chain of electrostatic blobs, as shown in Figure 1. The monomer segments within each blob behave as a random coil, with the degree of expansion being controlled by the solvent quality. Within each blob, the columbic electrostatic repulsion is balanced by the thermal energy. On length scales larger than each blob, electrostatics will be dominant, and the chain assumes the conformation of a rigid rod of blobs (Figure 1). As a function of solvency, the length of the chain, L, is given as

$$\begin{aligned} Nb\left(\frac{u}{A^2}\right)^{2/3}\tau^{-1} \qquad & T < \theta \\ L \sim Nb\left(\frac{u}{A^2}\right)^{1/3} \qquad & T = \theta \\ Nb\left(\frac{u}{A^2}\right)^{2/7} \qquad & T > \theta \end{aligned} \tag{1}$$

where u is the dimensionless ratio of the Bjerrum length to the monomer size and τ is the reduced temperature ($\tau = \theta - T/\theta$). In dilute solution, chains interact only through long-range Coulomb potentials. The characteristic length scale must therefore be equal to the spherical volume occupied by each chain, which has a radius equal to half the mean distance between the centers of neighboring chains. In polymer scaling terminology

$$R \sim V^{1/3} \sim \left(\frac{N}{c}\right)^{1/3} \tag{2}$$

where R is the radius, V is the volume, N is the number of monomer segments per polymer coil, and c is the concentration of monomer segments per unit volume.

As the concentration of polymer is increased, a condition is eventually reached where the polymer chains must become entangled and a network structure is developed. The onset of this entanglement defines the phase boundary between the dilute and semidilute concentration regimes. The critical concentration for overlap, c^*, is given as

$$c^* \sim \frac{N}{L^3} \sim B^3 b^{-3} N^{-2} \tag{3}$$

In the semidilute concentration regime, the distance between crossover points for the mesh structure defines the correlation length of this solution, as shown schematically in Figure 1. The concentration dependence of the correlation length, ξ, is described by the following scaling relationship:

$$\xi \sim \left(\frac{B}{cb}\right)^{1/2} \tag{4}$$

The correlation length and the electrostatic screening length both scale as $c^{-1/2}$ in the absence of added electrolyte.

3. Experimental Details

Materials. All water used here was of Millipore Milli-Q quality. The spheres used were 5 μm borosilicate glass particles (Duke Scientific). Spheres were used as supplied with no further treatment. Silica microscope slides (Escoproducts, Oak Ridge, New Jersey) were cleaned by soaking in 30 min in chromic acid, 30 min in concentrated hydrochloric acid, and 1 h in 100 mM sodium hydroxide solution. The polyelectrolyte, sodium poly(styrene sulfonate), was obtained from Polysciences Inc. (Warrington, Pennsylvania). The sample used here had a charge density of 100% and a nominal weight average molecular weight of 35 300 and a polydispersity index, Mw/Mn, of 1.01.

Methods. Interaction energy profiles between a single silica sphere and a microscope slide were determined using TIRM. This technique has been described in detail by a number of authors,[37−41] and only relevant details will be given here. An evanescent wave is generated at the solid/liquid interface by a total internally reflected laser light source within the glass slide. Any particle located close to the surface of the glass slide will scatter the incident evanescent wave. The scattering intensity is related to the distance between the sphere and the surface of the glass slide via

$$I(h) = I_0 \exp(-\beta h) \tag{5}$$

where β^{-1} is the decay length of the evanescent wave and I_0 is the "stuck" particle intensity, where the $h = 0$. Measuring the scattering intensity over time provides a histogram of the separation distances. The probability of finding a particle at any given separation distance, $\rho(h)$, is related to the total potential energy at that point through a Boltzmann relationship

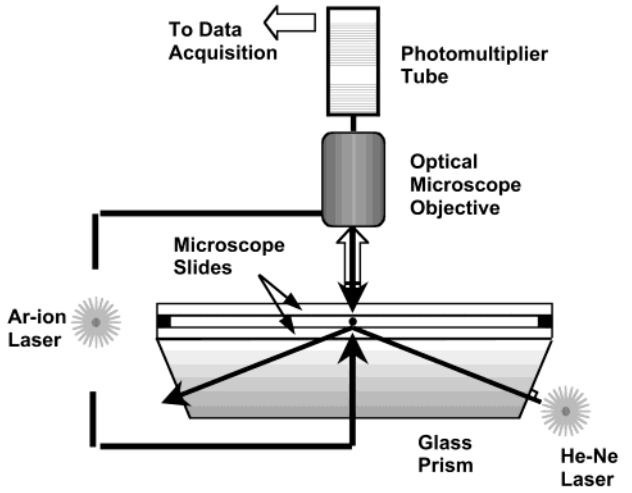

Figure 2. Schematic of the TIRM setup used here.

$$p(h) = A \exp\left(-\frac{\phi(h)}{kT}\right) \tag{6}$$

The potential energy profile is obtained by inverting this distribution. Full details are presented elsewhere.[40]

In a given experiment, the TIRM cell was initially filled with pH 10 water. Glass spheres were then introduced into the flow cell (see schematic in Figure 2). The evanescent wave with a decay length of 113.7 nm was produced using a 35 mW HeNe laser operating at 632 nm. A glass sphere of average brightness and size was selected and held in place using an optical tweezers while the rest of the particles were flushed form the cell with pH 10 water. The optical tweezers are generated using an argon ion laser (150 mW, $\lambda = 488$ nm) with the beam delivered from both above and below the sphere. The radiation pressure from the optical tweezers is also used to bias the height distribution of the particle of the slide, making the apparent weight decrease or increase depending on direction.

Once the excess particles have been pushed through the flow cell, the interaction energy of the glass sphere in pH 10 was recorded as a function of radiation pressure from below (decreasing the apparent weight of the sphere). Two to three hundred thousand intensity measurements were collected at 5 ms spacing between measurements through single photon counting using a PMT. The apparent weight of the particle is then determined by a function of radiation pressure and extrapolated to zero radiation pressure according to the method of Walz and Prieve.[37] The actual weight of the particle is then used to determine the diameter of the sphere.

The solution of interest was introduced in the flow cell while holding the particle in place with the optical tweezers. A minimum of 7−10 mL of fluid was used to change solutions (changing the volume of the fluid cell at least five times). Radiation pressure was then employed from either above, below, or both to ensure that the sphere sampled the largest number of elevations above the plate. The data collection procedure was the same as above. The solution can be changed in this manner for increasing concentrations of polymer. The last portion of the experiment is the distance calibration of the height data where the polymer solution is replaced with pH 10 water again and then a 10−15 mM sodium chloride solution is introduced to screen the repulsion levitating the particle. The particle will then come into contact with the plate (becoming "stuck"), and

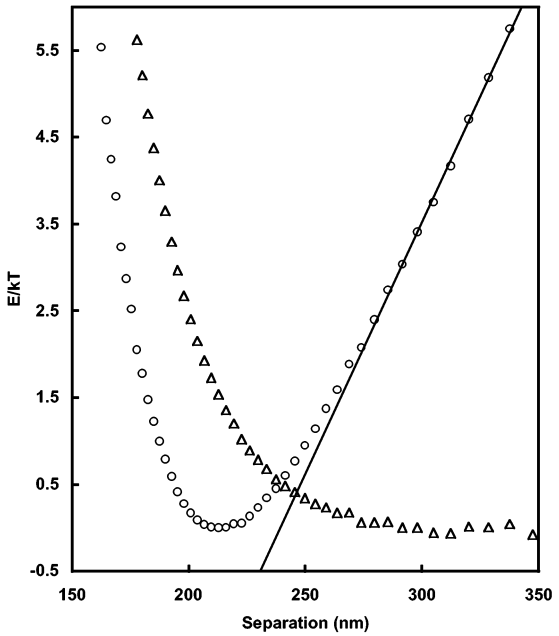

Figure 3. Measured potential energy profile between a 5 μm glass sphere and a silica plate in water at pH 10 with no added polyelectrolyte. Raw data of the interaction are given for the particle in a potential energy well formed by the gravitational and electrostatic components (○). The same data are also given after the net gravitational component has been subtracted from the raw profile (△). The calculated solution Debye length, κ^{-1}, from these data is 27 nm.

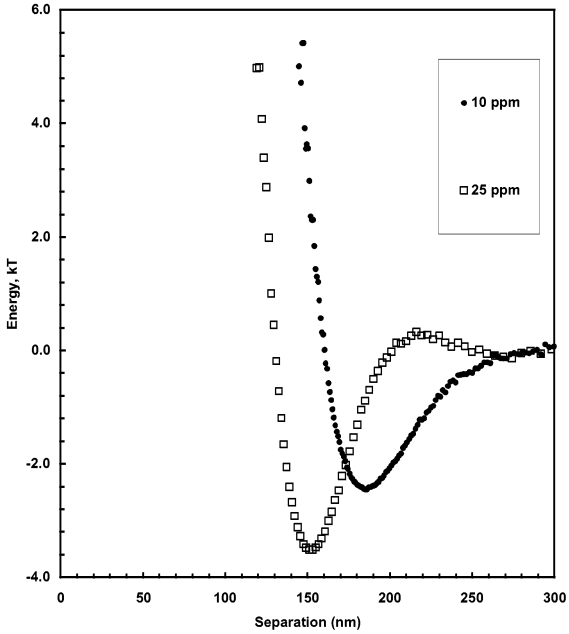

Figure 4. Potential energy profiles for the interaction of a 5 μm glass sphere with a flat silica plate in aqueous solutions of sodium poly(styrene sulfonate) [NaPSS] at two bulk concentrations as indicated in the figure. All measurements were performed at 25 °C and at a solution pH of 10.

the scattering intensity is recorded for 100 000 points. A region where there are no particles in the microscope field is then selected to determine the background scattering intensity. The difference between the average of the "stuck" particle intensity and the average of the background intensity is taken to be I_0 in eq 5.

4. Results and Discussion

The experiments performed in this investigation measured the interaction between two glass surfaces in various solutions of a nonadsorbing polyelectrolyte, sodium poly(styrene sulfonate) [NaPSS]. To ensure that there was no possibility of adsorption occurring, the experiments were performed at a solution pH of 10, where both the surfaces and the polymer are highly negatively charged.[14] Before discussing any results from this study, some relevant solution parameters for the polyelectrolyte will be presented.

In this work, we will assume that the polymer backbone, essentially polystyrene, is in a poor solvent condition. This is a significant, although not unreasonable, assumption in the case of NaPSS.[42] In aqueous solution at 25 °C, the Bjerrum length is 7 Å and hence $u = 2.3$. For highly charged NaPSS, a value of $A = 5$ and $\tau = 1$ have previously been determined.[36] Using these values in eq 1, along with $b = 3$ Å and $N = 160$, we determine a value of $L = 9.8$ nm for the sample used here. The chain overlap concentration, c^*, is determined from eq 3 to be approximately 6000 ppm. This value is in good agreement with data from neutron scattering experiments on similar polymers.[43] Thus, for the experiments reported here at concentrations of up to 1000 ppm, all data are expected to be collected in the dilute regime.

Raw data of the potential energy versus the surface-surface separation distance for the interaction of a single 5 μm glass sphere with a flat silica slide are shown in Figure 3. In a TIRM experiment, the motion of a particle, undergoing Brownian fluctuations, above a flat surface is recorded. The data shown in Figure 3 are typical of those measured in TIRM experiments[17−19,41] for surfaces interacting under the influence of a range of standard DLVO interaction forces. The potential energy well is bounded by a gravitational attraction at large separations and a long-range electrostatic repulsion at smaller separations. It is important in any TIRM experiment to collect data at sufficiently large separation distances, typically several Debye lengths above the minimum where the potential energy-separation curve becomes linear. A straight line fit to these data is used to allow a calculation of the particle's apparent weight. This is then used to allow a subtraction of the gravity component of the total energy from the profile. The result is a data set having the common form of an energy-separation profile that decays to zero at large surface−surface separation distances. The converted data set, after subtraction of the gravity component is also shown in Figure 3. The converted data illustrate the typical profiles seen for two charged surfaces interacting across an aqueous electrolyte solution. The main features of these data have been discussed in detail by a number of authors.[37−41,44] In this study, these data are simply used as a reference point for comparison to the data collected in the presence of the polyelectrolyte, and so no further discussion will be presented here.

The measured potential energy profiles between a single 5 μm glass sphere and a glass plate in the presence of poly(styrene sulfonate) [$M_w \sim 35\ 000$] at a range of concentrations, of between 10 and 1000 ppm, are shown in Figures 4−6. Before we discuss these data sets in detail, some comment on the experimental details and the consequences of the procedure for the results should be presented. In any TIRM experiment, accurate measurements of the relative energy levels at all points in a given profile can only be calculated if the complete profile was collected in a single experiment. For profiles of the type presented here, this means that the particle must sample all of the minima in a given profile spontaneously during a single experiment. When the barrier height between two minima becomes large (>10 kT), spontaneous movement between these

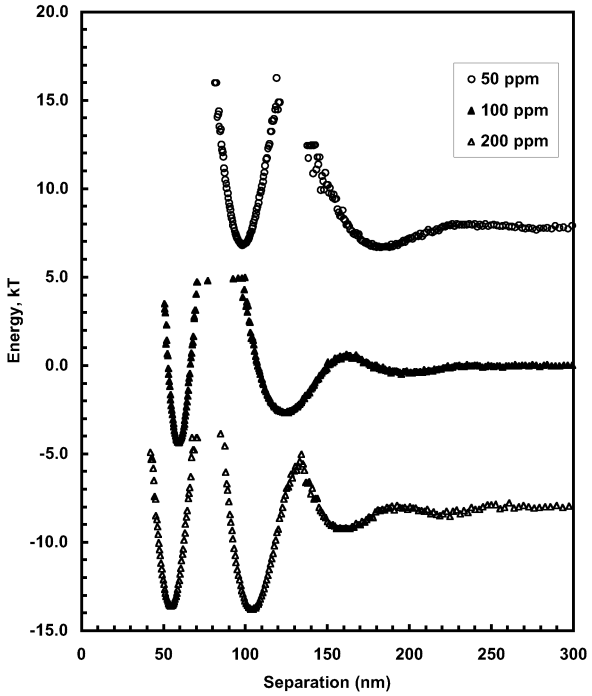

Figure 5. Potential energy profiles for the interaction of a 5 μm glass sphere with a flat silica plate in aqueous solutions of NaPSS at three bulk concentrations as indicated in the figure. All measurements were performed at 25 °C and at a solution pH of 10.

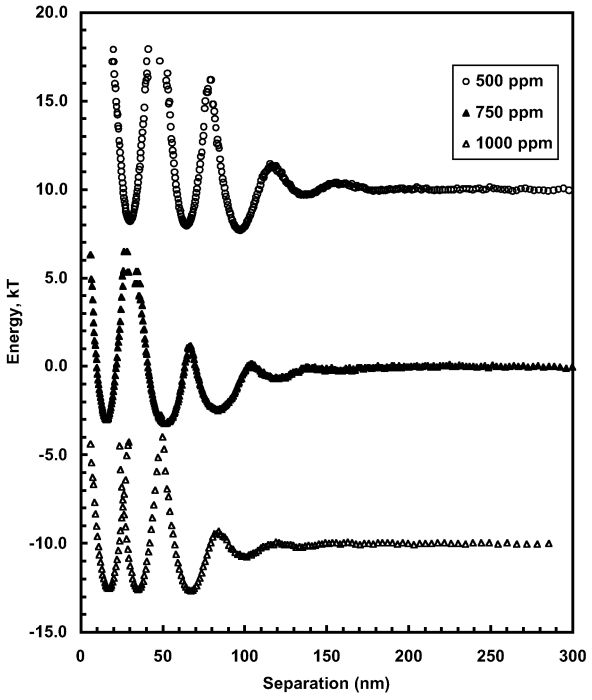

Figure 6. Potential energy profiles for the interaction of a 5 μm glass sphere with a flat silica plate in aqueous solutions of NaPSS at three bulk concentrations as indicated in the figure. All measurements were performed at 25 °C and at a solution pH of 10.

two minima is impossible. The consequences of this experimental limitation are important for data of the type presented here. At polymer concentrations of 100 ppm and below, the data presented accurately define both the positions and the relative energies of all minima in a given data set. For concentrations of 200 ppm and above, the presented data were collected in a set of consecutive experiments because when the particle entered one of the inner minima, at small separation distances, the height of the barrier for escape is too large. As an example, consider the data at 1000 ppm, shown in Figure 6. These data were collected in three experiments. Initially, data were collected by allowing the particle to approach the flat surface from a large separation distance. The data at separations of >50 nm were then collected in a single experiment. Entry into the minima at smaller separations was prevented by a significant energy barrier at around 50 nm separation. At the conclusion of this experiment, the same particle was "forced" into the minimum at $\sim$35 nm using radiation pressure. Because the walls of this minimum are large, escape was impossible. Thus, the relative energy of this well when compared to the zero position of the outer data set is unknown. However, the position of the well (separation distance) is still well characterized. Finally, the particle was forced into the energy well closest to the surface, again using radiation pressure. Once again, the position of this well is accurate but the relative energy is unknown.

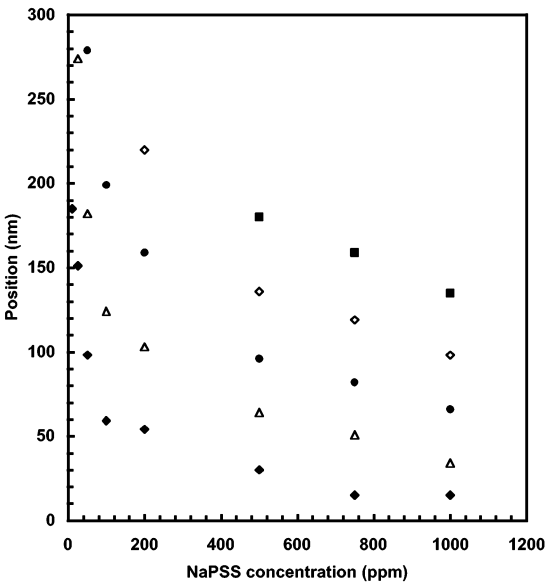

Figure 7. Plot of the positions of the potential energy minima versus polymer concentration.

At a solution pH of 10, no adsorption of the sodium poly(styrene sulfonate) is expected on either the sphere or the flat surface.[14] Close approach of the two surfaces should result in an attractive depletion interaction in addition to the standard electrical double layer and van der Waals components of the DLVO theory. The sensitivity of the TIRM technique is illustrated by the measurement of a depletion interaction at a bulk polymer concentration of only 10 ppm. The data shown in Figures 4−6 show that as the polymer concentration is increased the number of observable oscillations also increases. Furthermore, the position of the minima and the spacing between them are also concentration dependent. A plot of the minima position versus polymer concentration is shown in Figure 7. It is clear from this plot that, at polymer concentrations of above 500 ppm, up to 5 separate minima can be observed. Once again, this highlights the sensitivity of the TIRM approach for measurements of this type. In previously reported measurements of oscillatory interactions between surfaces in the presence of nonadsorbing particles, polymers or micelles, *a maximum* of only three minima were observed.[10,12,15,21−25] Furthermore, to observe these multiple minima, the solution concentration was raised well above the chain−chain overlap concentration into the semidilute polymer concentration regime.

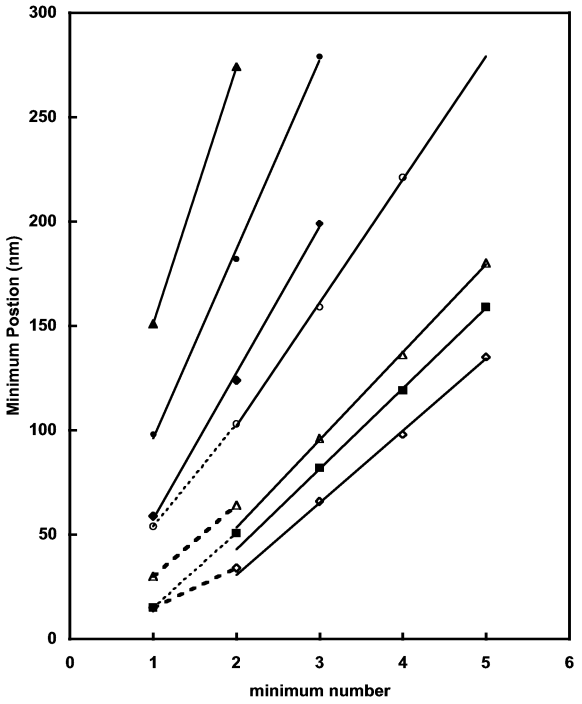

Figure 8. Plot of the minima positions as a function of the number of the minima. Minima, at any given polymer concentration, are numbered in an integral sequence starting with that minimum found at the smallest separation distance. For each polymer concentration, a line (or lines) of best fit through the data is presented. At concentrations of 200 ppm and above, the data are fitted using two straight-line relationships: one for the larger separation distances and the other for the final two minima.

From the data shown in Figures 4−6, each minimum was labeled with an increasing integer value starting at 1 for the minimum at the smallest separation distance. A plot of minima number versus separation distance is shown in Figure 8 for each concentration tested in this study where multiple minima could be seen. Starting from the largest separation distance at each concentration, a straight line fit was attempted to each data set. At all concentrations below 100 ppm polymer, a reasonable fit to the data was obtained for all minima. At concentrations of 100 ppm polymer and above, all data at large separations were well fitted by a straight line fit. However, the first minimum, and at higher concentrations the second, showed a significant deviation from these straight line fits. The linear correlation of these data at large separation distances indicates that, at all concentrations, the spacing between the minima is regular. The gradient of these best fit lines is therefore related to the spacing in the radial distribution of the polymer coils in dilute bulk solution. For a dilute solution of polyelectrolyte coils at low background electrolyte concentrations, we may expect an ordered space-filling, but nonintermixing latex, to form.[29] This is illustrated schematically in Figure 9. The spacing between polymer coils in such a system will be given by

$$D = L + m\kappa^{-1} \tag{7}$$

where D is the center-to-center distance between two coils, L is the characteristic rigid rod dimension, κ^{-1} is the Debye length, and m is a multiplier.

If such a nonintermixing latex does exist under dilute solution conditions, then the expected scaling relationship would be given by $\xi \sim c^{-1/3}$ (eq 2). A plot of the *minima spacings* as a function of polymer concentration is shown in Figure 10. The scaling exponent taken from a best fit to these data is −0.35, in excellent agreement with the predicted relationship.

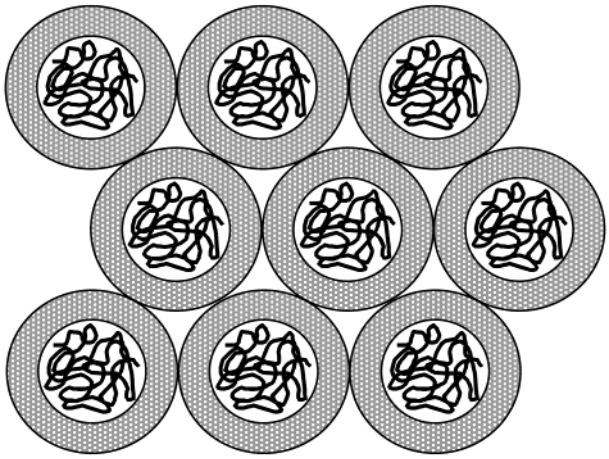

Figure 9. Schematic representation of a space filling latex of polymer chains (plus double layers) in dilute solution.

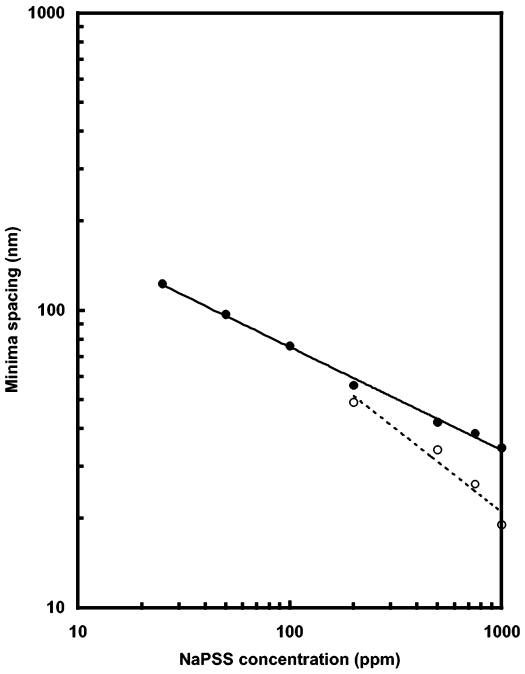

Figure 10. Dependence of the mean minimum−minimum spacing, derived from the gradients of the best fits to the data shown in Figure 8, as a function of the polymer concentration: (a) ●, gradient values at large separation distances; (b) ○, gradient values for the inner two minima at concentrations of 200 ppm and above. In both cases, the data are fitted using a scaling law relationship according to (a) $\xi = 372c_p^{-0.347}$; (b) $\xi = 996c_p^{-0.556}$.

TABLE 1: Calculated Values of *m* from eq 7

polymer concn (ppm)	centre-to-center distance, D (nm)	κ^{-1} (nm)	m
25	123	28	4.07
50	97	26	3.38
100	76	22	3.04
200	56	18	2.61
500	42	13	2.53
750	39	11	2.72
1000	35	9	2.88

Further evidence for the validity of the arrangement shown in Figure 9 may be found from calculations of the values of m (eq 7). These data are given in Table 1. The values of κ^{-1} are determined on the basis of the monomer concentration, a value of $A = 5$, and a pH of 10. The concentration of the macroion

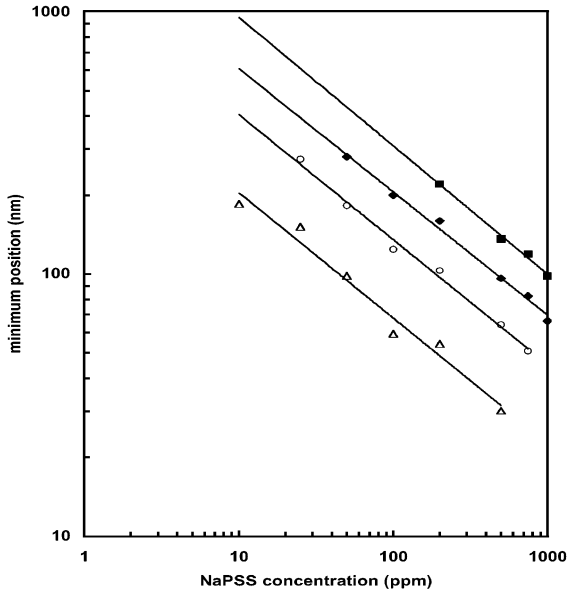

Figure 11. Plot of the absolute position of the potential energy minima as a function of the polymer concentration on a double logarithmic scale. The four data sets shown correspond to the 1st, 2nd, 3rd, and 4th measured minima at each concentration [see Figure 8]. Data are not shown for the inner minima at the highest concentrations, where significant deviation from "bulk" behavior is seen. A line of best fit to each data set indicates agreement with a scaling relation according to: (a) △, 1st minima, $\xi = 612c_p^{-0.478}$; (b) ○, 2nd minima, $\xi = 1211c_p^{-0.478}$; (c) ◆, 3rd minima, $\xi = 1785c_p^{-0.470}$; (d) ■, 4th minima, $\xi = 2932c_p^{-0.490}$.

is not included in these calculations because it's contribution is typically insignificant. Using these values and the value of L, the rigid rod length determined above, in eq 7, a value for m can be determined. At all but the two lowest concentrations, the calculated values of m are consistent and lie in the range 2.5−3. These data imply that the relevant chain dimensions controlling the periodicity of the oscillations is related to the rigid rod length plus 1−2 Debye lengths.

A plot of the *mimima positions* versus polymer concentration on a double logarithmic scale is given in Figure 11 for the first four sets of minima in Figure 8. Note that data are only given for minima that clearly correspond to the "bulk" behavior, i.e., large separation distances. For the four data sets analyzed, there is a consistent relationship that scales according to $c^{-1/2}$. This is directly related to an increase in electrical double layer screening with increased electrolyte concentration and suggests that the rigid rod dimensions are virtually independent of polymer concentration, as assumed.

Analysis of the *minima spacing* for the inner two minima at above 200 ppm polymer indicates a different functional relationship to those described above. A plot of the spacing, between the first and second minima, as a function of polymer concentration is also shown in Figure 10. The best fit to these data indicate a relationship that scales as $c^{-1/2}$ rather than the $c^{-1/3}$ that was predicted and observed at larger surface separations. This change in functional relationship may reflect a change in the packing of the polyelectrolyte chains close to the interface. Geometric considerations indicate that a close packed system of parallel chains should scale as $c^{-1/2}$ with increasing polymer concentration. It seems likely therefore that, at these higher polymer concentrations, one or perhaps two layers of the polyelectrolyte chains are lying parallel to the interface. This shrinking of the periodicity in the oscillations for the last layer of molecules is consistent with earlier experiments on concentrated particle dispersions.[45,46] The changed oscillatory character was then attributed to the self-organization of a monolayer of spheres parallel to the surface.

TABLE 2: Calculated Values of *m* in eq 7

polymer concn (ppm)	centre-to-center distance, D (nm)	κ^{-1} (nm)	m (using $L = 9$ nm)	m (using width = 2 nm)
200	49	18	2.22	2.61
500	34	13	1.92	2.46
750	26	11	1.54	2.18
1000	19	9	1.11	1.89

Values of the parameter m determined from the magnitude of the spacings, the value of L, and the values of κ^{-1} are given in Table 2. In this case, there is a general decrease in the magnitude of this value, approaching $m = 1$ at 1000 ppm. Such a result would imply that the effective electrolyte concentration is greater than the calculated value. The validity of this calculation is questionable, especially if the hypothesis of a parallel ordered layer is correct. In such a case, the characteristic dimension should be the "width" of the rod. This is expected to have a dimension of 1−2 nm. [12,18] The values of m have been recalculated using a rod width of 2 nm and are also given in Table 2. In these cases, the values of m range from 1.9 to 2.5. These values are reasonable if we assume that the activity of the electrolyte is not altering under confinement. Thus, the characteristic dimension is effectively the width of the rod plus 2 Debye lengths. It should also be noted that there is a decrease in the value of m as the concentration increases. This may reflect an increased restriction on the movement of the parallel ordered chains. The magnitude of the chain dimension within these short-range oscillations is comparable to earlier data obtained using the thin film balance[30] In this earlier work, the oscillations were interpreted as being due to a layer of polyelectrolyte molecules that were ordered parallel to the interface. It seems probable that a similar ordering of the polyelectrolyte is occurring here.

It is also apparent from the data presented here that there is a decrease in the apparent chain dimensions ($2m$) with increased polymer concentration. This decrease is due to a reduction in the molecular freedom of the individual polymer chains; that is, their motion is increasingly constrained at higher polymer concentrations. As the polymer concentration increases, the bulk osmotic pressure will result in a reduced tendency for the chains to escape the gap as the two surfaces approach one another. At polymer concentrations of below 200 ppm, no evidence for the parallel ordering of any layer confined between the surfaces was seen. This may be simply due to a lack of resolution preventing us from seeing multiple minima. However, it may also reflect a genuine lack of such order. At low polymer concentration and low added electrolyte, the extension of the double layer repulsion prevents close approach of any polymer chain to the surface. This limits the influence of the interface on chain ordering.

Current theoretical understanding of structural correlations for dilute solutions of flexible polyelectrolytes are based upon chain-chain interactions that arise from long-range electrostatic potentials.[35] These repulsive potentials between the particles or chains result in a regular distribution of their centers of mass on a periodic lattice. Such interactions for highly charged species can lead to the formation of colloidal crystal structures, as have been previously seen for charged particles.[47] The structuration of the solution is then expected to lead to a peak in the structure factor, $S(q)$, that corresponds either to solidlike or liquidlike order depending upon the strength of the interaction relative to kT, the thermal energy. Any peak in the structure factor must

correspond to an oscillatory radial distribution function, $g(r)$. If two surfaces are then brought together across such a solution, oscillatory force interactions may be expected. These forces arise as a result of the disruption of the bulk order during the approach of the surfaces. However, it is important to note that they do not arise from a surface-induced structuration phenomenon. The data presented here confirm that dilute polyelectrolyte solutions in low electrolyte conditions do exhibit strong structural correlations. The increased number of oscillations and their increased amplitude with increasing polymer concentration reflects the increase in order within the system as the volume fraction of chains increases. The influence of a surface on the structural order of the solution is profound. On the basis of the measured data, it appears that the presence of an interface can cause a local parallel alignment of the chains.

The oscillatory interactions observed here can be compared with recent theoretical predictions for the oscillatory interactions caused by structural correlations within a depletant polymer solution.[8,46,48] The periodicity of the oscillations is predicted to scale as $C_p^{-1/3}$ in the dilute concentration regime. Interestingly, it has also been predicted in one case that the amplitude of the oscillatory interactions will decrease with increasing polymer concentration;[48] the amplitude of the oscillations was seen to increase with concentration here, in agreement with earlier experimental and theoretical data.[21−25] The presence of oscillatory interactions indicates clearly that there are solution structural correlations. These correlations have been predicted to show liquidlike order in bulk solution, as is observed here. Furthermore, the presence of bulk order is then expected to be perturbed at a surface resulting in a liquidlike layering as is seen for hard spheres or Lennard-Jones fluids. The results here present the first unequivocal evidence that this is also seen for solutions of polyelectrolytes in the dilute concentration regime.

5. Conclusions

The potential energies of interaction between a single glass sphere and a flat glass surface in the presence of a nonadsorbing polyelectrolyte, NaPSS, have been measured directly using the TIRM technique. Upon close approach of the surfaces, a measurable depletion interaction is observed at concentrations of NaPSS as low as 10 ppm. As the polymer concentration is increased, up to a maximum concentration of 1000 ppm, an increasingly apparent oscillatory interaction is observed. The amplitude of the oscillations was observed to decay with increasing surface−surface separation. At the highest polymer concentration examined here, up to six oscillations were observed. Analysis of the periodicity of these oscillations indicated that at relatively large surface−surface separations the dilute polyelectrolyte system behaves as a nonintermixing latex. The concentration dependence of the oscillatory period follows a scaling relation given by $\xi \sim c^{-1/3}$, in direct agreement with theoretical predictions. At polymer concentrations of greater than 200 ppm, a significant deviation from this scaling relation was seen for the final two oscillations. This was attributed to a confinement-induced ordering of the "rigid" polyelectrolyte chains parallel to the interface. The experimental data presented here are the first direct measurements of the bulk solution order for a dilute highly charged polyelectrolyte (in low electrolyte conditions). In addition, the importance of confinement induced ordering of the polyelectrolytes is also demonstrated.

Acknowledgment. S.B. is grateful to The University of Newcastle for the award of funded Sabbatical leave and to the Center for Complex Fluids Engineering of Carnegie-Mellon University for financial support of this research project. R.R.D. would like to acknowledge financial support from the Shell Graduate Fellowship.

References and Notes

(1) Napper, D. H. *Polymeric Stabilisation of Colloidal Dispersions*; Academic Press: London, 1983.
(2) Fleer, G. J.; Scheutjens, J. M. H. M.; Cohen-Stuart, M. A.; Cosgrove, T.; Vincent, B. *Polymers at Interfaces*; Chapman and Hall: London, 1993.
(3) Asakura, S.; Oosawa, F. *J. Chem. Phys.* **1954**, *22*, 1255.
(4) Fleer, G. J.; Scheutjens, J. M. H. M.; Vincent, B. Polymer Adsorption and Dispersion Stability. *ACS Symp. Ser.* **1984**, *240*, 245.
(5) de Gennes, P. G. *Macromolecules* **1981**, *14*, 1637.
(6) Vincent, B. *Colloids Surf.* **1990**, *50*, 241.
(7) Feigin, R. I.; Napper, D. H. *J. Colloid Interface Sci.* **1979**, *7*, 117.
(8) van der Gucht, J.; Besseling, N. A. M.; van Male, J.; Cohen-Stuart, M. A. *J. Chem. Phys.* **2000**, *113*, 2886.
(9) Dautzenberg, H.; Jaeger, W.; Kötz, J.; Philipp, B.; Seidel, C.; Stscherbina, D. *Polyelectrolytes*; Hanser: Munich, Germany 1994.
(10) Richetti, P.; Kékicheff, P. *Phys. Rev. Lett.* **1992**, *68*, 1951.
(11) Milling, A.; Biggs, S. *J. Colloid Interface Sci.* **1995**, *170*, 604.
(12) Milling, A. *J. Phys. Chem. B.* **1996**, *100*, 8986.
(13) Milling, A.; Vincent, B. *J. Chem. Soc., Faraday Trans.* **1997**, *93*, 3179.
(14) Burns, J. L.; Yan, Y.-D.; Jameson, G. J.; Biggs, S. *Colloids Surf.* **2000**, *162*, 265.
(15) Milling, A.; Kendall, K. *Langmuir* **2000**, *16*, 5106.
(16) Biggs, S.; Burns, J. L.; Yan, Y.-D.; Jameson, G. J.; Jenkins, P. *Langmuir* **2000**, *16*, 9242.
(17) Sharma, A.; Walz, J. Y. *J. Chem. Soc., Faraday Trans.* **1996**, *92*, 4997.
(18) Sharma, A.; Tan, S. N.; Walz, J. Y. *J. Colloid Interface Sci.* **1997**, *191*, 236.
(19) Odiachi, P. C.; Prieve, D. C. *Colloids Surf.* **1999**, *146*, 315.
(20) Asakura, S.; Oosawa, F. *J. Polym. Sci.* **1958**, *33*, 183.
(21) Dickman, R.; Attard, P.; Simonian, V. *J. Chem. Phys.* **1997**, *107*, 205.
(22) Gotzelmann, B.; Evans, R.; Dietrich, S. *Phys. Rev. E.* **1998**, *57*, 6785.
(23) Bechinger, C.; Rudhardt, D.; Leiderer, P.; Roth, R.; Dietrich, S. *Phys. Rev. Lett.* **1999**, *83*, 3960.
(24) Crocker, J. C.; Matteo, J. A.; Dinsmore, A. D.; Yodh, A. G. *Phys. Rev. Lett.* **1999**, *82*, 4352.
(25) Ohshima, Y. N.; Sakagami, H.; Okumoto, K.; Tokoyoda, A.; Igarashi, T.; Shintaku, K. B.; Toride, S.; Sekino, H.; Kabuto, K.; Nishio, I. *Phys. Rev. Lett.* **1997**, *78*, 3963.
(26) de Gennes, P. G.; Pincus, P.; Velasco, R. M.; Brochard, F. *J. Phys. (Paris)* **1976**, *37*, 1461.
(27) Bergeron, V.; Langevin, D.; Asnacios, A. *Langmuir* **1996**, *12*, 1550.
(28) Asnacios, A.; Espert, A.; Colin, A.; Langevin, D. *Phys. Rev. Lett.* **1997**, *78*, 4974.
(29) Klitzing, R. v.; Espert, A.; Colin, A.; Langevin, D. *Colloids Surf.* **2001**, *176*, 109.
(30) Kolaric, B.; Jaeger, W.; Klitzing, R. v. *J. Phys. Chem. B* **2000**, *104*, 5096.
(31) Théodoly, O.; Tan, J. S.; Ober, R.; Williams, C. E.; Bergeron, V. *Langmuir* **2001**, *17*, 4910.
(32) Claesson, P. M.; Dedinaite, A.; Blomberg, E.; Sergeyev, V. G. *Ber. Bunsen-Ges. Phys. Chem.* **1996**, *100*, 1008.
(33) Claesson, P. M.; Dedinaite, A.; Blomberg, E.; Sergeyev, V. G. *Prog. Colloid Polym. Sci.* **1997**, *106*, 224.
(34) The scattering wave vector q is given by the equation, $q = 4\pi/\lambda \sin(\theta/2)$, where λ is the wavelength, θ is the scattering angle, and n_0 is the refractive index of the scattering medium.
(35) Barrat, J.-L.; Joanny, J.-F. *Adv. Chem. Phys.* **1996**, *94*, 1.
(36) Dobrynin, A. V.; Colby, R. H.; Rubinstein, M. *Macromolecules* **1995**, *28*, 1859.
(37) Walz, J. Y.; Prieve, D. C. *Langmuir* **1992**, *8*, 3043.
(38) Prieve, D. C.; Walz, J. Y. *Appl. Opt.* **1993**, *32*, 1629.
(39) Prieve, D. C.; Frej, N. A. *Langmuir* **1990**, *6*, 396.
(40) Prieve, D. C. *Adv. Colloid Interface Sci.* **1999**, *82*, 93.
(41) Bevan, M. A.; Prieve, D. C. *Langmuir* **1999**, *15*, 7925.
(42) Dobrynin, A. V.; Rubinstein, M. *Macromolecules* **1999**, *32*, 915.
(43) Kassapidou, K.; Jesse, W.; Kuil, M. E.; Lapp, A.; Egelhaaf, S.; van der Maarel, J. R. C. *Macromolecules* **1997**, *30*, 2671.
(44) Pagac, E. S.; Tilton, R. D.; Prieve, D. C. *Langmuir* **1998**, *14*, 5106.
(45) Nikolov, A. D.; Wasan, D. T. *Langmuir* **1992**, *8*, 2985.
(46) Trokhymchuk, A.; Henderson, D.; Nikolov, A.; Wasan, D. T. *Langmuir* **2001**, *17*, 4940.
(47) Hachisu, S.; Kobayashi, Y.; Kose, A. *J. Colloid Interface Sci.* **1973**, *42*, 342.
(48) Yethiraj, A. *J. Chem. Phys.* **1999**, *111*, 1797.